

## SOFTWARE METAPAPER

# PIVlab – Towards User-friendly, Affordable and Accurate Digital Particle Image Velocimetry in MATLAB

William Thielicke<sup>1</sup> and Eize J. Stamhuis<sup>2</sup><sup>1</sup> Department of Ocean Ecosystems, University of Groningen, The Netherlands; Department of Biomimetics, Bremen University of Applied Sciences, Germany; Biomimetics-Innovation-Centre, Bremen University of Applied Sciences, Germany<sup>2</sup> Biomimetics-Innovation-Centre, Bremen University of Applied Sciences, Germany

Digital particle image velocimetry (DPIV) is a non-intrusive analysis technique that is very popular for mapping flows quantitatively. To get accurate results, in particular in complex flow fields, a number of challenges have to be faced and solved: The quality of the flow measurements is affected by computational details such as image pre-conditioning, sub-pixel peak estimators, data validation procedures, interpolation algorithms and smoothing methods. The accuracy of several algorithms was determined and the best performing methods were implemented in a user-friendly, GUI based open-source tool for performing DPIV flow analysis in MATLAB.

**Keywords:** particle image velocimetry; PIV; MATLAB; fluid dynamics; flow analysis; direct cross correlation; discrete Fourier transform; sub-pixel peak finding; window deformation; interpolation; histogram equalization

## (1) Overview

### Introduction

Digital particle image velocimetry (DPIV) is a common technique for non-intrusive, quantitative and qualitative flow visualization. A number of research articles deals with the implementation and optimization of the DPIV technique [1–8]. Here, a GUI-based open-source tool (PIVlab) for DPIV analyses in MATLAB (MathWorks, Natick, Massachusetts) is presented. The tool takes advantage of several built-in MATLAB features, and eases subsequent data processing by providing a close link to the popular MATLAB user interface.

In DPIV, the motion of a fluid (either gaseous or liquid) is visualized by illuminating a thin sheet of fluid containing reflective and neutrally buoyant tracer particles. A digital image sensor is positioned parallel to the illuminated sheet, capturing the movement of the particles (see **Figure 1**). In most DPIV analyses, two images (A and B) of the illuminated plane are captured at  $t_0$  and  $t_0 + \Delta t$ . Velocities in the sheet can hence be derived from  $\Delta t$  and the distance that the particles travelled from image A to B (particle displacement). In DPIV, the particle displacement is calculated for groups of particles by evaluating the cross-correlation of many small sub-images (interrogation areas). The correlation yields the most probable displacement for a group of particles travelling on a straight line between image A and image B [8].

### Implementation and architecture

PIVlab is programmed in MATLAB and additionally requires the image processing toolbox to run. The main file is 'PIVlab\_GUI.m'. It contains all GUI-related program parts

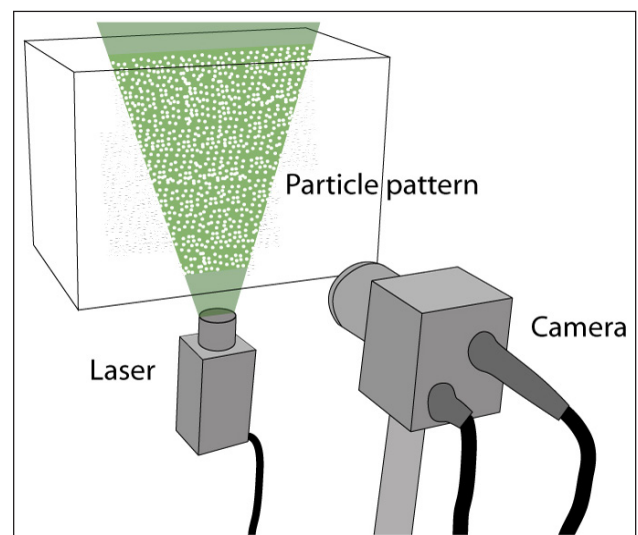


**Figure 1:** Principle of DPIV: A laser sheet illuminates the particles contained in the fluid. A high-speed camera records the displacement of the particle pattern.

and most of the functions that are accessible from the GUI. The most important functions for performing a PIV analysis (pre-processing: 'PIVlab\_preproc.m'; cross-correlation: 'piv\_FFTmulti.m' and 'piv\_DCC.m') are also accessible from the command line (see example in 'PIVlab\_commandline.m') when the user desires to automate the whole process or to include it in another application.

A DPIV analysis typically consists of three main steps (image pre-processing, image evaluation, post-processing,

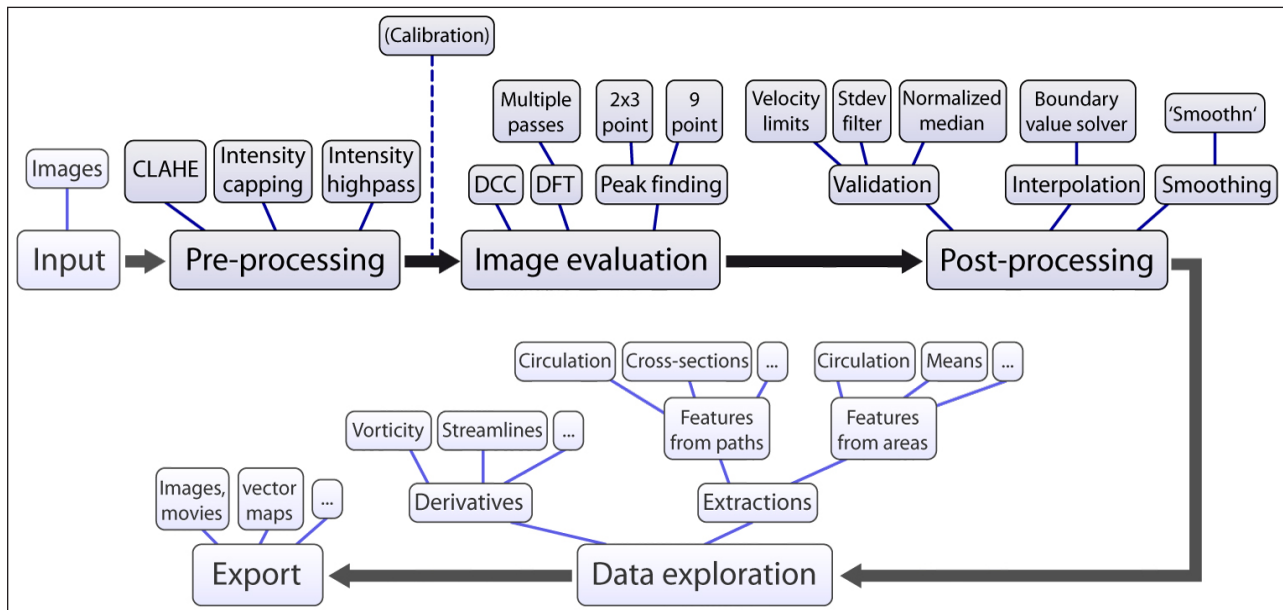


**Figure 2:** DPIV analyses in PIVlab. Overview of the workflow and the implemented features that are presented in the next sections.

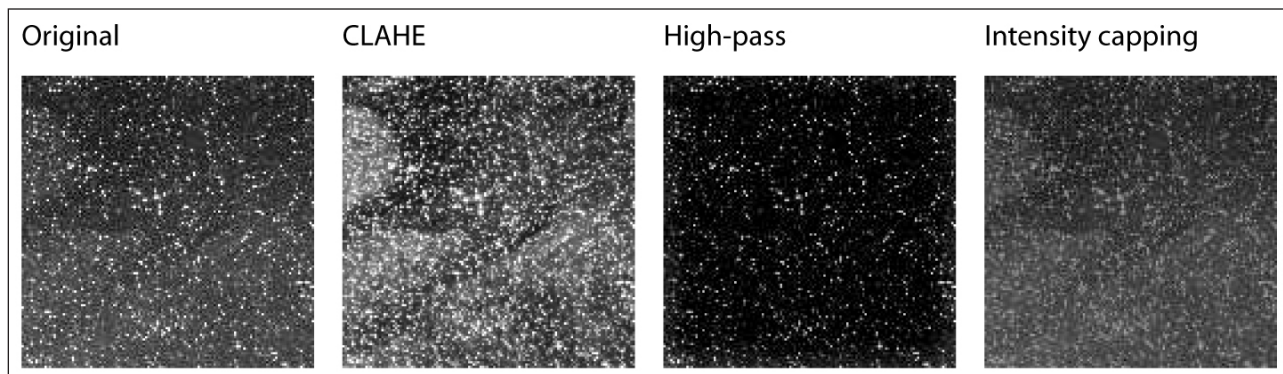


**Figure 3:** The effect of several pre-processing techniques, see text for a description.

see **Figure 2**). All of these steps are accessible from the GUI of PIVlab. The workflow is menu-based, starting at the left with image input and pre-processing options, and then continuing to the right of the menu (image evaluation / PIV analysis, post-processing, data exploration). This workflow is demonstrated in tutorials and screen capture videos that can be found on the project website.

The following section will give an overview of the relevant features and techniques that are accessible in PIVlab:

### **Image pre-processing**

One common approach to improve the measurement quality is the enhancement of images before the actual image correlation takes place [8, 9]. This section presents a selected number of pre-processing techniques that are implemented in PIVlab (see **Figure 3** for examples).

#### **Histogram equalization**

Contrast limited adaptive histogram equalization (CLAHE) was developed to increase the readability of image data in medical imaging [10]. CLAHE operates on small regions (tiles) of the image: In every tile, the most frequent intensities of the image histogram are spread out to the full

range of the data (from 0 to 255 in 8-bit images). Regions with low exposure and regions with high exposure are therefore optimized independently. CLAHE significantly improves the probability of detecting valid vectors in experimental images by  $4.7 \pm 3.2\%$  [9].

#### **Intensity highpass**

Inhomogeneous lighting can cause low frequency background information which can be removed by applying a high-pass filter that mostly conserves the high frequency information from the particle illumination [11]. The filter emphasizes the particle information in the image, and suppresses any low frequency information in the images (including all low frequency displacement information).

#### **Intensity capping**

The DPIV method assumes that all particles within an interrogation window have the same motion. This will not be the case in reality, as perfectly uniform flow does hardly exist. Bright particles or bright spots within the area will contribute statistically more to the correlation signal, which may bias the result in non-uniform flows [9]. The intensity capping filter circumvents this problem. An

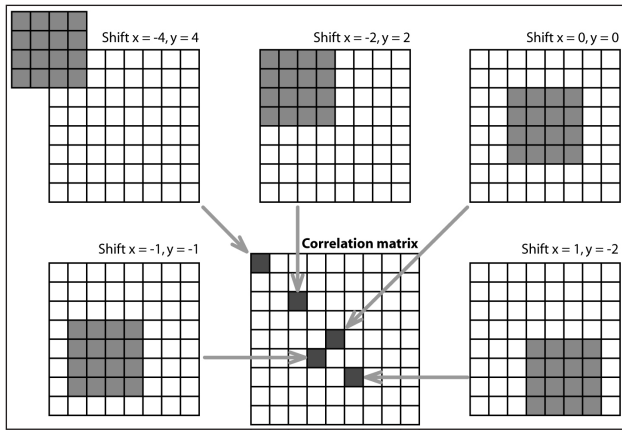


**Figure 4:** Calculation of the correlation matrix using DCC as it is performed in MATLAB. Interrogation area A (size 4-4 pixels) is correlated with interrogation area B (size 8-8 pixels) and yields the correlation matrix (size 9-9 pixels). Adapted from [8].

upper limit of the greyscale intensity is selected, and all pixels that exceed the threshold are replaced by this upper limit. Therefore, unlike CLAHE, only a small amount of the pixel intensity information is adjusted, limiting the potential negative impact of image modifications [9]. Intensity capping improves the probability of detecting valid vectors in experimental images by  $5.2 \pm 2.5\%$  [9].

### Image evaluation

The most sensitive part of a DPIV analysis is the cross correlation algorithm: Small sub images (interrogation areas) of an image pair are cross correlated to derive the most probable particle displacement in the interrogation areas. In essence, the cross-correlation is a statistical pattern matching technique that tries to find the particle pattern from interrogation area A back in interrogation area B. This statistical technique is implemented with the discrete cross correlation function [12]:

$$C(m,n) = \sum_i \sum_j A(i,j)B(i-m,j-n) \quad (1)$$

where A and B are corresponding interrogation areas from image A and image B.

The location of the intensity peak in the resulting correlation matrix  $C$  gives the most probable displacement of the particles from A to B [12].

There are two common approaches to solve equation 1: The most straightforward approach is to compute the correlation matrix in the spatial domain (see **Figure 4** for a graphical representation of this correlation). This approach is either called direct cross correlation [13], particle image pattern matching [12], or convolution filtering [14].

Another approach is to compute the correlation matrix in the frequency domain (discrete Fourier transform, DFT). The DFT is calculated using a fast Fourier transform [15]. Both approaches are implemented in PIVlab as they both have advantages as well as some drawbacks; these will be presented in short in the next sections. More details on the mathematical background of cross correlation can be found elsewhere (e. g. [8, 16]).

### Direct cross correlation (DCC)

The direct cross correlation computes the correlation matrix in the spatial domain. In DCC, the interrogation areas A and B can have two different sizes [14]. When B is chosen twice as large as A, a particle displacement of up to half the size of A will not result in any loss of information and provide a reliable correlation matrix with low background noise (see **Figure 4**, top middle and **Figure 5**, top). DCC has been shown to create more accurate results than a standard DFT approach [12]. The disadvantage of DCC is the increased computational cost with respect to a standard DFT approach, especially with large interrogation areas [8, 12, 15].

Discrete Fourier transform (DFT) and advanced DFT techniques  
The potential drawback of DCC – the computational cost – can be resolved by calculating the correlation matrix in the frequency domain [8] using FFT (see **Figure 6A**). This approach uses interrogation areas of identical size; therefore every particle displacement induces some loss of information, which can be noticed by the increasing amount of background noise in the correlation matrix (see **Figure 5**, bottom). This background noise complicates the detection of the intensity peak and decreases accuracy. It is therefore advisable to reduce the displacement to about one quarter of the interrogation area, in order to keep the background noise in the correlation matrix low [1].

This disadvantage can be offset by running several passes of the DFT on the same dataset [18]: The integer result of the first analysis pass is used to offset the interrogation area in the following passes. The loss of information due to particle displacement is hence minimized. The interrogation grid can be refined with every pass [19], yielding a high spatial resolution in the final vector map, together with a high dynamic velocity range and an optimal signal to noise ratio.

In real flows, the particle patterns will additionally be sheared and rotated; the non uniform particle motion will broaden the intensity peak in the correlation matrix and deteriorate the result. Several methods that account for the transformation of the interrogation areas have been proposed [20–22]. In PIVlab, the following procedure is implemented: The analysis is started with a regular DFT analysis. The first pass yields displacement information at the centre of each interrogation area. When the areas overlap one another by e. g. 50%, there is additional displacement information at the borders and corners of each interrogation area (nine positions in total, see **Figure 6B**, left). This information is used to calculate displacement information at every pixel of the interrogation areas via bilinear interpolation. Next, interrogation area B is deformed according to this displacement information (see **Figure 6B**, right) using either bilinear interpolation (faster) or spline interpolation (higher precision, but slower). The next interrogation pass correlates the original interrogation area A with the deformed area B. The remaining displacement information of each pass is accumulated. After a few passes, the displacement has been determined with high accuracy. Between the passes, but not after the final

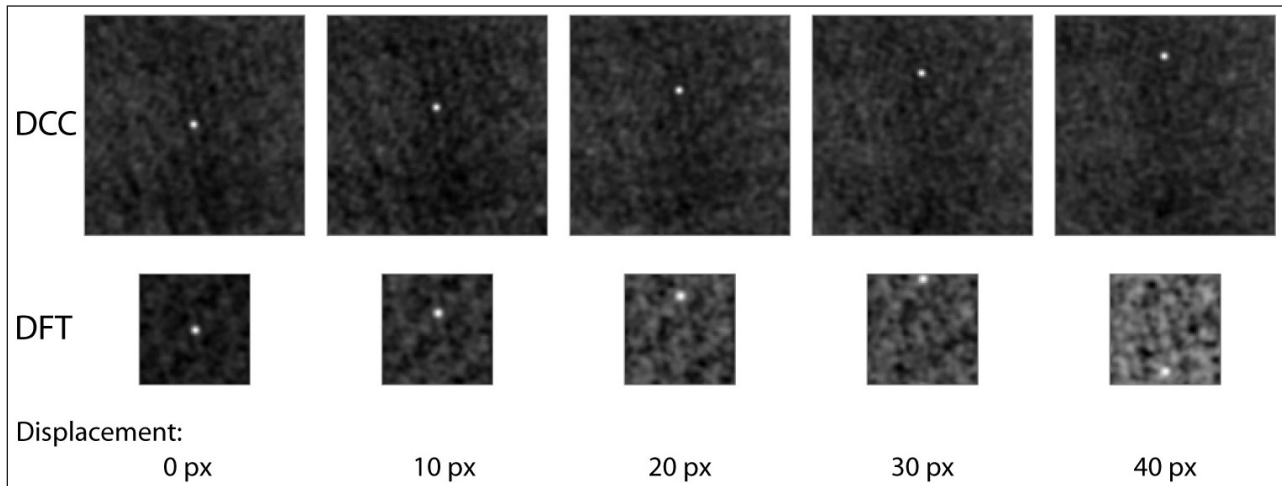


**Figure 5:** Correlation matrices of the DCC (top) and the DFT approach (bottom), interrogation area A is 64·64 pixels for both DCC and DFT. Area B is 128·128 pixels in DCC and 64·64 pixels in DFT. In DCC, the background noise does not increase up to a displacement of 32 pixels. In DFT, background noise immediately increases if the displacement is larger than 0 pixels. A displacement of more than 32 pixels will flip the correlation peak to the opposite side of the correlation matrix, and thus makes correct measurements impossible.

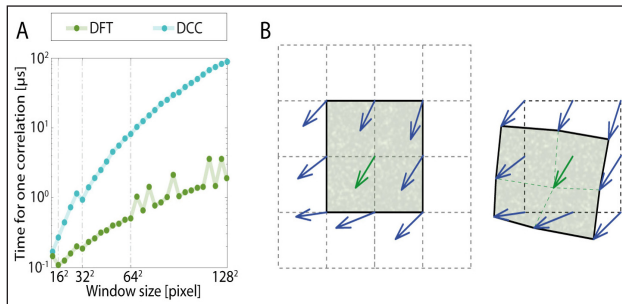


**Figure 6: A:** Calculation speed of DCC in comparison with DFT (both calculations performed in MATLAB). For the FFT calculations, FFTW is used [17] which accepts inputs of arbitrary size, but is slow for sizes that are prime or which have large prime factors (note the peaks in the graph). Generally, the DFT approach is much faster. **B:** Principle of the window deformation technique. Left: After the first interrogation pass, displacement information is present at nine positions inside the interrogation area. This information is interpolated to derive the displacement of every pixel of the interrogation area. Subsequently, interrogation area B is deformed, followed by several additional interrogation passes.

pass, the velocity information is smoothed and validated and missing information is interpolated. Data validation can be relatively strict, as any deteriorating effect of interpolation and smoothing will be corrected in the correlation of the following pass.

#### Peak finding

The choice of the peak finding technique is – similar to the choice of the cross correlation technique – another important factor for the accuracy of DPIV. The integer displacement of two interrogation areas can be determined straightforward from the location of the intensity peak of the correlation matrix. The location can be refined with

sub-pixel precision using a range of methods [8, 23, 24]. The standard procedure is to fit a Gaussian function to the integer intensity distribution (see **Figure 7**). It is sufficient to use only the directly adjacent vertical and horizontal pixels (two times a 3-point fit = 2·3-point fit) and to evaluate the x and y axis separately. The peak of the fitted function is used to determine the particle displacement with sub-pixel precision.

If the particle displacement within an interrogation area is exposed to shear or rotation or if the images suffer from excessive motion blur, the displacement peak may have an elliptical shape [8]. In this case, a two-dimensional Gaussian function (9-point fit) has a better performance [25]. The added value of using a two-dimensional Gaussian function is more pronounced in non-deforming methods, such as DCC and single pass DFT. Both peak finding algorithms are implemented in PIVlab.

#### Post-processing

##### Data validation

Post processing of DPIV data is generally required to obtain reliable results [26]. A basic method to filter outliers in PIVlab is to choose limits for acceptable velocities manually. Velocity thresholds can also be determined semi automatically by comparing each velocity component with a lower threshold and an upper threshold ( $t_{lower}$  and  $t_{upper}$ ):

$$t_{lower} = \bar{u} - n * \sigma_u \quad (2)$$

$$t_{upper} = \bar{u} + n * \sigma_u \quad (3)$$

where  $u$  = mean velocity;  $\sigma_u$  = standard deviation of  $u$ .

The user defined value of  $n$  determines the strictness of this filter. This filter works very well in practice, as it adapts to some extent to the nature of the flow.

A more universal outlier detection method that automatically adapts to local flow situations is the normalized median test [27] (or local median filter). The filter evaluates



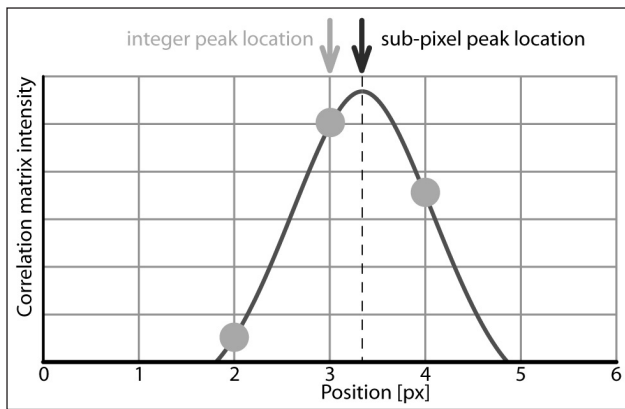


**Figure 7:** Principle of the Gaussian 2-3-point fit: Sub-pixel precision is achieved by fitting a one-dimensional Gaussian function (solid line) to the integer intensity distribution of the correlation matrix (dots) for both axes independently (only one axis is shown here).

the velocity fluctuation with respect to the median in a 3-3 neighbourhood around a central vector. The median of this fluctuation is then used as normalization for a more classical median test.

#### Data interpolation

After the removal of outliers, missing vectors should be replaced by interpolated data [26]. One common technique is the 3-3 neighbourhood (3-3 mean) interpolation. Two-dimensional linear or spline interpolation [5] are other alternatives. PIVlab uses a boundary value solver for interpolation<sup>1</sup>. The approach provides an interpolation that is generally fairly smooth, and over larger regions with missing data, it will tend towards the average of the boundary velocities, which prevents overshooting.

#### Data smoothing

A certain amount of measurement noise will be inevitable in DPIV analyses [8]. Noise can be effectively reduced by applying data smoothing. Raffel et al. [8] propose to perform a convolution of the data with a 2-2 or 3-3 kernel with equal weights. Another common and effective method to smooth DPIV data is median filtering [8]. More advanced smoothing algorithms are based on a penalized least squares method [28] – the latter technique is implemented in PIVlab.

#### Data exploration

Many DPIV studies reveal very complex flow patterns. Such a complexity is hard to describe purely with vector maps. The strength of PIVlab is that it offers a large number of possibilities to further process and distil the results: Derivatives, such as vorticity and divergence can be calculated, data can be extracted from paths or areas and integral quantities can be calculated comfortably.

#### Quality control

Functional testing has been performed on Windows XP and Windows 7 with MATLAB releases R2010a, R2011a and R2013b. Although the authors do not have access to

additional operation systems and MATLAB versions, the reports from many users claim that PIVlab works flawlessly on Mac OS X and UNIX/Linux too. Bugs that have been discovered in some of the last ten PIVlab releases have been corrected before the next release. The user acceptance of PIVlab has been monitored and optimized while the software was used by more than 150 supervised students with several different operating systems and MATLAB releases.

Furthermore, extensive tests on the quality of the results obtained with PIVlab were performed using more than  $6 \cdot 10^4$  synthetic particle images. The image properties were modified in a way that allowed to calculate the accuracy of all important PIV image parameters according to [8]. Detailed results of these tests are reported in [29]<sup>2</sup>. Furthermore, the PIVlab toolbox contains a script that performs a fully automatic analysis of the accuracy of the DPIV analysis: The script 'Accuracy.m' will generate random PIV images, evaluate these images, and perform a comparison between the calculated and the real displacement of the interrogation areas. This script helps users to make sure that PIVlab works accurately on their combination of MATLAB and operating system.

#### Accuracy of the DPIV analyses

The quality of the DPIV measurements in PIVlab was extensively evaluated using synthetic particle images with known properties. The effect of particle image diameter, particle density, sensor noise, particle pair loss, motion blur and shear was determined and is reported in detail elsewhere [29]<sup>2</sup>. These quality tests revealed that DFT using window deformation outperforms the basic DCC and DFT correlation, especially under challenging conditions. The additional computational load is compensated by the increased robustness and accuracy of the algorithm. Under optimal conditions (particle image diameter  $\approx 3$  pixels, particle density  $\approx 5 - 15$  particles/window, no noise, no particle pair loss, no motion blur, no shear) the bias error of the window deformation DPIV algorithms is smaller than 0.005 pixels and the random error is below 0.02 pixels.

#### Interpolation performance

The performance of the most popular interpolation techniques and the boundary value solver are tested: A number of real and synthetic image pairs are analyzed using standard DPIV (see **Figure 8**, left). An increasing amount of random vectors (0% to 15%) is removed from the resulting vector matrix (see **Figure 8**, middle). The missing data is interpolated using one of the interpolators (see **Figure 8**, right), and finally, the mean absolute difference between the original data and the interpolated data is determined. This whole procedure is repeated 1000 times for each image pair and each level of missing data. Under challenging conditions and large amounts of missing data, the boundary value solver which is implemented in PIVlab performs best (see **Figure 9**). More detail is given in [29].

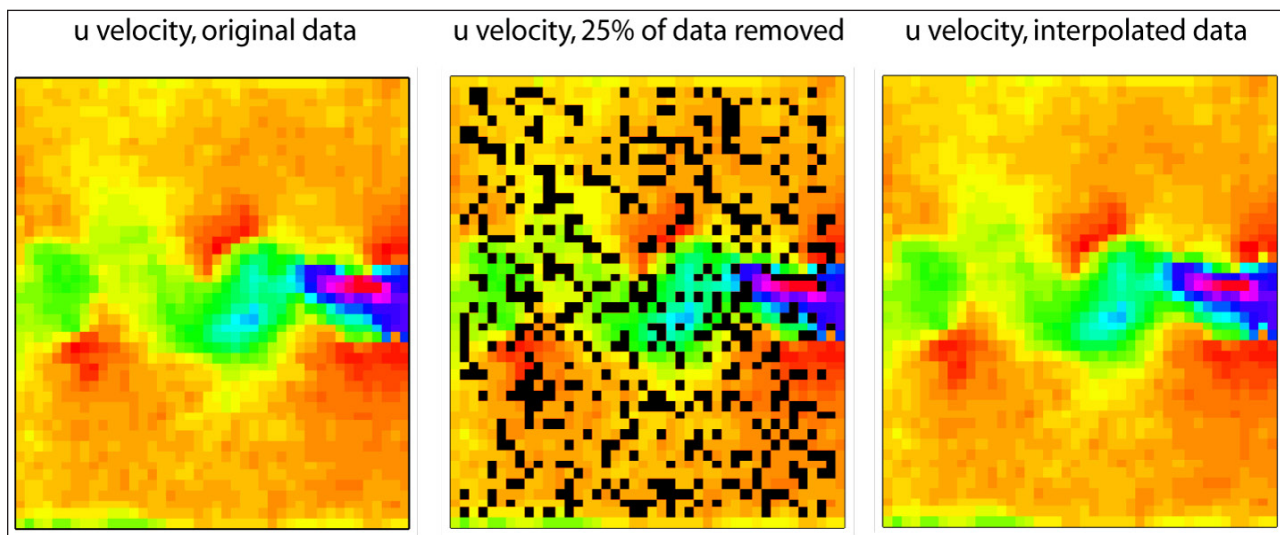


**Figure 8:** Procedure for testing several interpolation techniques. Left: Original velocity data. Middle: Data is removed at random positions. Right: Gaps are filled with interpolation and compared to the original velocity data.

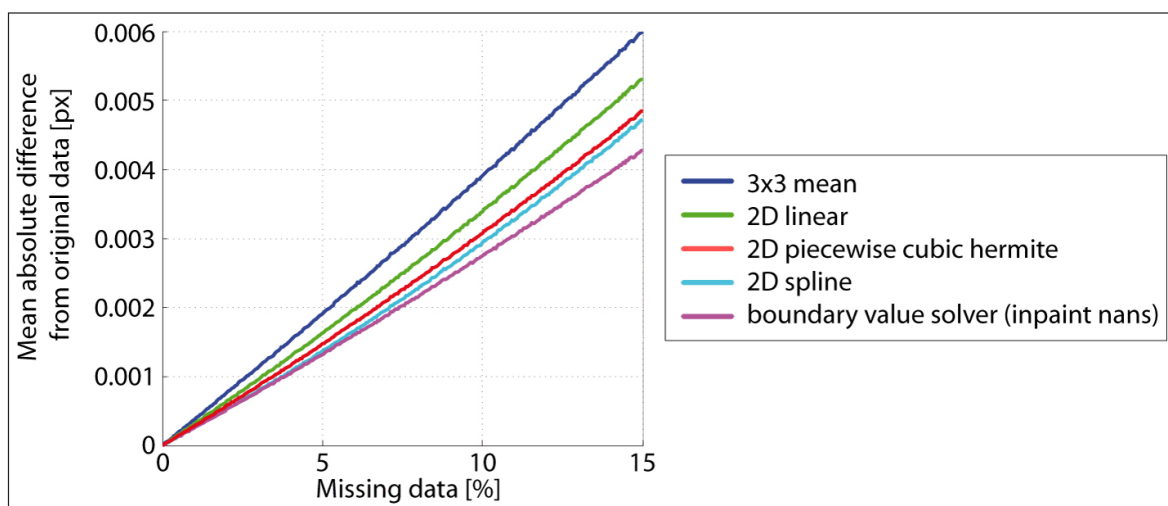


**Figure 9:** Performance of popular interpolators. The boundary value solver performs best under the presence of larger amounts ( $> 10\%$ ) of missing data.  $n = 1000$ .

### Smoothing performance

The performance of the smoothing algorithms is tested using DPIV data of synthetic particle images (more detail is given in [29]). Data smoothing – no matter what algorithm is used – always decreases the amount of noise introduced by the DPIV algorithm and hence increases the quality of the velocity estimation (see **Figure 10**). The application of the 'Smoothn' algorithm [28] reduces the difference between analysis and true velocities. It was therefore decided to implement this algorithm in PIVlab in order to further enhance the accuracy of the velocity estimation.

### Support

Support is available through the website of PIVlab (<http://PIVlab.blogspot.com>), where questions can be posted and generally receive quick responses from the authors. The email address for support requests is also noted on this website. It furthermore contains news, tips, updates and tutorials for PIVlab users.

## (2) Availability

### Operating system

Based on MATLAB 7.10.0 (R2010a): Windows, UNIX/Linux, Macintosh

### Programming language

MATLAB 7.10.0 (R2010a), upward compatible

### Additional system requirements

MATLAB 7.10.0 (R2010a): 1 GB disk space, 1 GB RAM

### Dependencies

MATLABs Image Processing Toolbox is required

### List of contributors

WT: Programming of the tool and the graphical user interface (GUI); selection, implementation and evaluation of the algorithms; writing this article; support and maintenance of the tool.

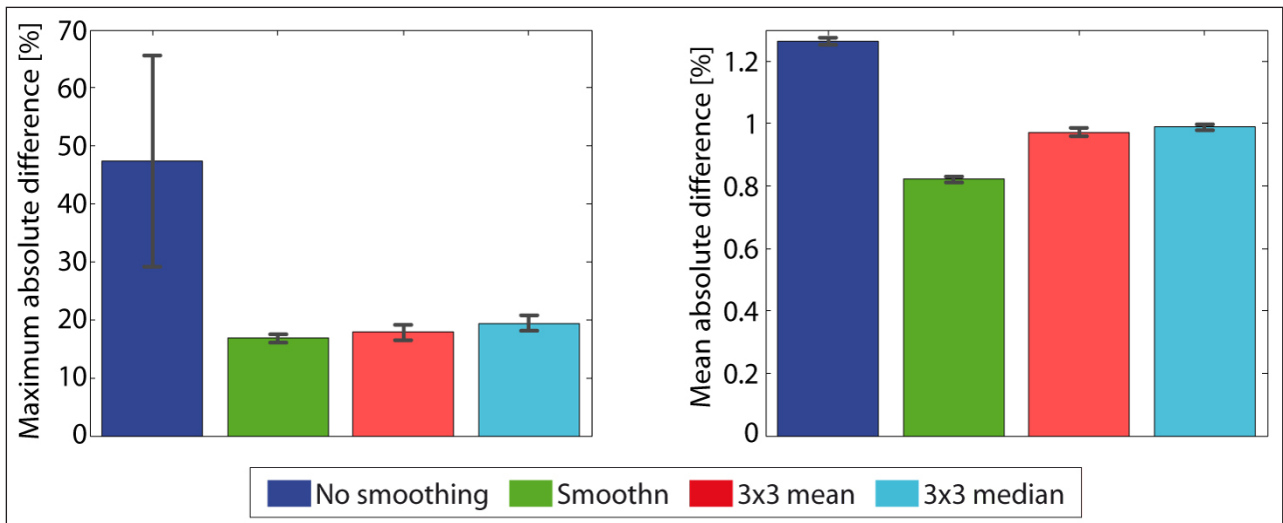


**Figure 10:** Validation of smoothing algorithms. Left: Maximum absolute difference between the calculated velocities and the true velocities in percent of the maximum true velocity. Right: Mean absolute difference.  $n=250$ .

EJS: Support with the layout of both the tool and the GUI; feedback, tips and discussions on the functionality.

#### Archive

##### Name

Figshare.com

##### Persistent identifier

<http://dx.doi.org/10.6084/m9.figshare.1092508>

##### Licence

CC-BY

##### Publisher

William Thielicke

##### Date published

03/07/2014

##### Language

English

### (3) Reuse potential

The analysis of flow velocities is an integral part of many research disciplines. Here, DPIV has become a very popular method. The development of user-friendly, accurate and free DPIV tools greatly enhances the practicability and availability of this technique. In many cases, it can even be sufficient to use low cost digital cameras and lasers to study complex flows with PIVlab (e. g. [30]). The simple graphical user interface of PIVlab enables users that are new to the field of DPIV to generate accurate results quickly.

PIVlab has proved its value in a number of research projects. The tool has been used for 'conventional' measurements of fluid velocities, but also in a very different context, for example flow visualizations within cells, echocardiographic velocimetry of the human heart and deformation of sand and gravel [29, 31–54].

PIVlab can be extended with custom functionalities and features using MATLABs GUI editor and many of MATLABs pre-built functions. It is e. g. the basis of 'PTVlab', an independent software tool that was designed to track particles. Individual functions of PIVlab (e. g. the image correlation code) can be used for custom projects.

PIVlab is highly integrated with MATLAB and benefits from MATLABs extensive plotting and data handling features. But data can also be exported to generic ASCII files, which can be processed e. g. with Excel (Microsoft, Redmond, WA). As PIVlab can also export to binary vtk files, Paraview (Kitware, Inc., Clifton Park, NY) is another very appropriate possibility to visualize and explore the flow data.

#### Acknowledgements

See <http://www.mathworks.com/matlabcentral/fileexchange/27659>

#### Notes

- <sup>1</sup> inpaint\_nans by John D'Errico, <http://www.mathworks.com/matlabcentral/fileexchange/4551-inpaintnans>
- <sup>2</sup> The accuracy tests are part of the PIVlab documentation and they are made available on the website of our tool (<http://PIVlab.blogspot.com>)

#### References

1. Keane, R. D. & Adrian, R. J. 1990 Optimization of particle image velocimeters. i. double pulsed systems *Measurement Science and Technology* **1**, 1202–1215. DOI: <http://dx.doi.org/10.1088/0957-0233/1/11/013>
2. Adrian, R. J. 1991 Particle-imaging techniques for experimental fluid mechanics *Annual Review of Fluid Mechanics* **23**, 261–304. DOI: <http://dx.doi.org/10.1146/annurev.fl.23.010191.001401>
3. Willert, C. E. & Gharib, M. 1991 Digital particle image velocimetry *Experiments in Fluids* **10**, 181–193. DOI: <http://dx.doi.org/10.1007/BF00190388>

4. **Buchhave, P.** 1992 Particle image velocimetry - status and trends *Experimental Thermal and Fluid Science* **5**, 586–604. DOI: [http://dx.doi.org/10.1016/0894-1777\(92\)90016-X](http://dx.doi.org/10.1016/0894-1777(92)90016-X)
5. **Stamhuis, E. J. & Videler, J. J.** 1995 Quantitative flow analysis around aquatic animals using laser sheet particle image velocimetry *Journal of Experimental Biology* **198**, 283–294.
6. **Willert, C.** 1996 The fully digital evaluation of photographic piv recordings *Applied Scientific Research* **56**, 79–102. DOI: <http://dx.doi.org/10.1007/BF02249375>
7. **Grant, I.** 1997 Particle image velocimetry: A review Proceedings of the Institution of Mechanical Engineers, Part C: Journal of Mechanical Engineering Science **211**, 55–76. DOI: <http://dx.doi.org/10.1243/0954406971521665>
8. **Raffel, M., Willert, C., Wereley, S. & Kompenhans, J.** 2007 *Particle Image Velocimetry* Springer 2 edn.
9. **Shavit, U., Lowe, R. & Steinbuck, J.** 2007 Intensity capping: a simple method to improve cross-correlation piv results *Experiments in Fluids* **42**, 225–240. DOI: <http://dx.doi.org/10.1007/s00348-006-0233-7>
10. **Pizer, S. M., Amburn, E. P., Austin, J. D., Cromartie, R., Geselowitz, A., Greer, T., ter Haar Romeny, B., Zimmerman, J. B. & Zuiderveld, K.** 1987 Adaptive histogram equalization and its variations *Computer Vision, Graphics, and Image Processing* **39**, 355–368 DOI: [http://dx.doi.org/10.1016/S0734-189X\(87\)80186-X](http://dx.doi.org/10.1016/S0734-189X(87)80186-X)
11. **Gonzalez, R. C. & Wintz, P.** 1987 *Digital image processing* Addison-Wesley Publishing Company, Inc.
12. **Huang, H., Dabiri, D. & Gharib, M.** 1997 On errors of digital particle image velocimetry *Measurement Science and Technology* **8**, 1427–1440. DOI: <http://dx.doi.org/10.1088/0957-0233/8/12/007>
13. **Okamoto, K., Nishio, S., Saga, T. & Kobayashi, T.** 2000 Standard images for particle-image velocimetry *Measurement Science and Technology* **11**, 685–691. DOI: <http://dx.doi.org/10.1088/0957-0233/11/6/311>
14. **Stamhuis, E. J.** 2006 Basics and principles of particle image velocimetry (piv) for mapping biogenic and biologically relevant flows *Aquatic Ecology* **40**, 463–479. DOI: <http://dx.doi.org/10.1007/s10452-005-6567-z>
15. **Soria, J.** 1996 An investigation of the near wake of a circular cylinder using a video-based digital cross-correlation particle image velocimetry technique *Experimental Thermal and Fluid Science* **12**, 221–233. DOI: [http://dx.doi.org/10.1016/0894-1777\(95\)00086-0](http://dx.doi.org/10.1016/0894-1777(95)00086-0)
16. **Keane, R. & Adrian, R.** 1992 Theory of cross-correlation analysis of piv images *Applied Scientific Research* **49**, 191–215. DOI: <http://dx.doi.org/10.1007/BF00384623>
17. **Frigo, M. & Johnson, S. G.** 2005 The design and implementation of FFTW3 *Proceedings of the IEEE* **93**, 216–231. DOI: <http://dx.doi.org/10.1109/JPROC.2004.840301>
18. **Westerweel, J., Dabiri, D. & Gharib, M.** 1997 The effect of a discrete window offset on the accuracy of cross-correlation analysis of digital piv recordings *Experiments in Fluids* **23**, 20–28. DOI: <http://dx.doi.org/10.1007/s003480050082>
19. **Scarano, F. & Riethmuller, M. L.** 1999 Iterative multigrid approach in piv image processing with discrete window offset *Experiments in Fluids* **26**, 513–523. DOI: <http://dx.doi.org/10.1007/s003480050318>
20. **Huang, H., Fiedler, H. & Wang, J.** 1993 Limitation and improvement of piv, part ii: Particle image distortion, a novel technique *Experiments in Fluids* **15**, 263–273.
21. **Jambunathan, K., Ju, X. Y., Dobbins, B. N. & Ashforth-Frost, S.** 1995 An improved cross correlation technique for particle image velocimetry *Measurement Science and Technology* **6**, 507–514. DOI: <http://dx.doi.org/10.1088/0957-0233/6/5/012>
22. **Scarano, F. & Riethmuller, M. L.** 2000 Advances in iterative multigrid piv image processing *Experiments in Fluids* **29**, S051–S060. DOI: <http://dx.doi.org/10.1007/s003480070007>
23. **Lourenco, L. & Krothapalli, A.** 1995 On the accuracy of velocity and vorticity measurements with piv *Experiments in Fluids* **18**, 421–428. DOI: <http://dx.doi.org/10.1007/BF00208464>
24. **Roesgen, T.** 2003 Optimal subpixel interpolation in particle image velocimetry *Experiments in Fluids* **35**, 252–256. DOI: <http://dx.doi.org/10.1007/s00348-003-0627-8>
25. **Nobach, H. & Honkanen, M.** 2005 Two-dimensional gaussian regression for sub-pixel displacement estimation in particle image velocimetry or particle position estimation in particle tracking velocimetry *Experiments in Fluids* **38**, 511–515. DOI: <http://dx.doi.org/10.1007/s00348-005-0942-3>
26. **Nogueira, J., Lecuona, A. & Rodriguez, P. A.** 1997 Data validation, false vectors correction and derived magnitudes calculation on piv data *Measurement Science and Technology* **8**, 1493. DOI: <http://dx.doi.org/10.1088/0957-0233/8/12/012>
27. **Westerweel, J. & Scarano, F.** 2005 Universal outlier detection for piv data *Experiments in Fluids* **39**, 1096–1100. DOI: <http://dx.doi.org/10.1007/s00348-005-0016-6>
28. **Garcia, D.** 2010 Robust smoothing of gridded data in one and higher dimensions with missing values *Computational Statistics and Data Analysis* **54**, 1167–1178. DOI: <http://dx.doi.org/10.1016/j.csda.2009.09.020>
29. **Thielicke, W.** 2014 *The Flapping Flight of Birds – Analysis and Application* Ph.D. thesis Rijksuniversiteit Groningen.
30. **Ryerson, W. G. & Schwenk, K.** 2012 A simple, inexpensive system for digital particle image velocimetry (dpiv) in biomechanics *Journal of*




- Experimental Zoology* **317**, 127–140. DOI: <http://dx.doi.org/10.1002/jez.725>
31. **Leong, T., Collis, J., Manasseh, R., Ooi, A., Novell, A., Bouakaz, A., Ashokkumar, M. & Kentish, S.** 2011 The role of surfactant headgroup, chain length, and cavitation microstreaming on the growth of bubbles by rectified diffusion *The Journal of Physical Chemistry* **115**, 24310–24316. DOI: <http://dx.doi.org/10.1021/jp208862p>
  32. **Booth-Gauthier, E., Alcoser, T., Yang, G. & Dahl, K.** 2012 Force-induced changes in subnuclear movement and rheology *Biophysical Journal* **103**, 2423–2431. DOI: <http://dx.doi.org/10.1016/j.bpj.2012.10.039>
  33. **Jiang, Y.-J. & Towhata, I.** 2012 Experimental study of dry granular flow and impact behavior against a rigid retaining wall *Rock Mechanics and Rock Engineering* 1–17.
  34. **Piro, V., Piro, N. & Piro, O.** 2012 Characterization of intraventricular blood flow using a micro-bubble-contrast tracking echo-piv technique *Journal of the American College of Cardiology* **59**, E1139–E1139. DOI: [http://dx.doi.org/10.1016/S0735-1097\(12\)61140-1](http://dx.doi.org/10.1016/S0735-1097(12)61140-1)
  35. **Roy, A., Metaxas, A. & Ross, T.** 2012 Swimming patterns of larval strongylocentrotus droebachiensis in turbulence in the laboratory *Marine Ecology Progress Series* **453**, 117–127. DOI: <http://dx.doi.org/10.3354/meps09662>
  36. **Sanchez, T., Chen, D. T. N., DeCamp, S. J., Heymann, M. & Dogic, Z.** 2012 Spontaneous motion in hierarchically assembled active matter *Nature* **491**, 431–434. DOI: <http://dx.doi.org/10.1038/nature11591>
  37. **Simmons, C. S., Ribeiro, A. & Pruitt, B. L.** 2013 Formation of composite polyacrylamide and silicone substrates for independent control of stiffness and strain *Lab Chip* **13**, 646–649. DOI: <http://dx.doi.org/10.1039/c2lc41110e>
  38. **Todaro, M. C., Choudhuri, I., Belohlavek, M., Jahangir, A., Carerj, S., Oreto, L. & Khandheria, B. K.** 2012 New echocardiographic techniques for evaluation of left atrial mechanics *European Heart Journal - Cardiovascular Imaging* **13**, Advance access973–984.
  39. **Cambau, T., Hure, J. & Marthelot, J.** 2013 Local stresses in the janssen granular column *Physical Review E* **88**, 022204.
  40. **Chen, Z., Jiang, C. & Nepf, H.** 2013 Flow adjustment at the leading edge of a submerged aquatic canopy *Water Resources Research* **49**, 5537–5551. DOI: <http://dx.doi.org/10.1002/wrcr.20403>
  41. **Datta, S. S., Chiang, H., Ramakrishnan, T. S. & Weitz, D. A.** 2013 Spatial fluctuations of fluid velocities in flow through a three-dimensional porous medium *Phys. Rev. Lett.* **111**, 064501. DOI: <http://dx.doi.org/10.1103/PhysRevLett.111.064501>
  42. **Eriksson, I., Powell, J. & Kaplan, A.** 2013 Melt behavior on the keyhole front during high speed laser welding *Optics and Lasers in Engineering* **51**, 735–740. DOI: <http://dx.doi.org/10.1016/j.optlaseng.2013.01.008>
  43. **Hartmann, A., Stamp, M., Kmeth, R., Buchegger, S., Stritzker, B., Saldamli, B., Burgkart, R., Schneider, M. F. & Wixforth, A.** 2013 A novel tool for dynamic cell adhesion studies - the de-adhesion number investigator dani *Lab Chip*. DOI: <http://dx.doi.org/10.1039/C3LC50916H>
  44. **Miller, J., Michael, J., Slipchenko, M., Roy, S., Meyer, T. & Gord, J.** 2013 Simultaneous high-speed planar imaging of mixture fraction and velocity using a burst-mode laser *Applied Physics B* **113**, 93–97. DOI: <http://dx.doi.org/10.1007/s00340-013-5665-1>
  45. **Panciroli, R. & Porfiri, M.** 2013 Evaluation of the pressure field on a rigid body entering a quiescent fluid through particle image velocimetry *Experiments in Fluids* **54**, 1–13. DOI: <http://dx.doi.org/10.1007/s00348-013-1630-3>
  46. **Senatore, C., Wulfmeier, M., VlahiniÄž, I., Andrade, J. & Iagnemma, K.** 2013 Design and implementation of a particle image velocimetry method for analysis of running gear-soil interaction *Journal of Terramechanics* **50**, 311–326. DOI: <http://dx.doi.org/10.1016/j.jterra.2013.09.004>
  47. **Shi, Q., Ghosh, R. P., Engelke, H., Rycroft, C. H., Cassereau, L., Sethian, J. A., Weaver, V. M. & Liphardt, J. T.** 2013 Rapid disorganization of mechanically interacting systems of mammary acini *Proceedings of the National Academy of Sciences*. DOI: <http://dx.doi.org/10.1073/pnas.1311312110>
  48. **Sun, C.-I. & Hsiao, T.-h.** 2013 On the background design for microscale background-oriented schlieren measurements of microfluidic mixing *Microfluidics and Nanofluidics* 1–17. DOI: <http://dx.doi.org/10.1007/s10404-013-1309-3>
  49. **Taddeucci, J., Valentine, G. A., Sonder, I., White, J. D. L., Ross, P.-S. & Scarlato, P.** 2013 The effect of pre-existing craters on the initial development of explosive volcanic eruptions: an experimental investigation *Geophysical Research Letters* **40**, 507–510. DOI: <http://dx.doi.org/10.1002/grl.50176>
  50. **Wang, C., Qiu, S. & Eliasson, V.** 2013 Quantitative pressure measurement of shock waves in water using a schlieren-based visualization technique *Experimental Techniques* **Early View**. DOI: <http://dx.doi.org/10.1111/ext.12068>
  51. **Zhou, B., Fraser, K. H., Poelma, C., Mari, J.-M., Eckersley, R. J., Weinberg, P. D. & Tang, M.-X.** 2013 Ultrasound imaging velocimetry: Effect of beam sweeping on velocity estimation *Ultrasound in Medicine & Biology* **39**, 1672–1681. DOI: <http://dx.doi.org/10.1016/j.ultrasmedbio.2013.03.003>
  52. **Bloch, G., Kuczaty, J. & Sattelmayer, T.** 2014 Application of high-speed digital holographic interferometry for the analysis of temperature distributions and velocity fields in subcooled flow boiling *Experiments in Fluids* **55**, 1–12. DOI: <http://dx.doi.org/10.1007/s00348-014-1678-8>

53. **Jalalisendi, M., Pancioli, R., Cha, Y. & Porfiri, M.** 2014 A particle image velocimetry study of the flow physics generated by a thin lamina oscillating in a viscous fluid *Journal of Applied Physics* **115**, 054901 <http://dx.doi.org/10.1063/1.4863721>
54. **Schlüßler, R., Czarske, J. & Fischer, A.** 2014 Uncertainty of flow velocity measurements due to refractive index fluctuations *Optics and Lasers in Engineering* **54**, 93–104. DOI: <http://dx.doi.org/10.1016/j.optlaseng.2013.10.011>

**How to cite this article:** Thielicke, W and Stamhuis, E J 2014 PIVlab – Towards User-friendly, Affordable and Accurate Digital Particle Image Velocimetry in MATLAB. *Journal of Open Research Software*, 2: e30, DOI: <http://dx.doi.org/10.5334/jors.bl>

**Published:** 16 October 2014

**Copyright:** © 2014 The Author(s). This is an open-access article distributed under the terms of the Creative Commons Attribution 3.0 Unported License (CC-BY 3.0), which permits unrestricted use, distribution, and reproduction in any medium, provided the original author and source are credited. See <http://creativecommons.org/licenses/by/3.0/>.

 *Journal of Open Research Software* is a peer-reviewed open access journal published by Ubiquity Press.

OPEN ACCESS 